APPLICATION OF A HIGH PRESSURE MICROBOMB TO HYDROSTATIC PRESSURIZATION OF MAGNETITE

Thesis for the Degree of M.S.

MICHIGAN STATE UNIVERSITY

JOHN KELLY MAHER

1977

ABSTRACT

APPLICATION OF A HIGH PRESSURE MICROBOMB TO HYDROSTATIC PRESSURIZATION OF MAGNETITE

Ву

John Kelly Maher

This thesis presents a study of hydrostatic pressure effects on the remanent magnetization of magnetite. Two types of samples were used; a single crystal of magnetite, and a synthetic "rock" composed of a resin matrix and a powder of synthetic magnetite.

The samples were initially saturated in a 2 kilogauss field, then pressurized to 4.0 kilobars in an oil-filled non-magnetic chamber. Isothermal remanent magnetization was measured during pressurization by means of a ballistic magnetometer. Pressure was increased and decreased in a continuous cycle during the tests.

During the first pressurization, the sample magnetization dropped to about 70% of the initial saturation magnetization with a pressure of 1.5 kilobars, and continued to drop at a slower rate to about 55% of the initial saturation with a pressure of 3.0 kilobars. Pressure was reduced to 2.0 kilobars with no further change in magnetization, then increased to 4.0 kilobars with another 5% drop in magnetization to about 50% of the initial value.

The thesis also presents some alterations made in a high pressure microbomb used by earlier researchers (Carmichael, et. al., 1968). The paper discusses both the development and use of the bomb and the complimentary apparatus required for pressurization and magnetic measurements. The latter includes a ballistic magnetometer specifically designed by R.S. Carmichael for use with this system.

ACKNOWLEDGEMENTS

I would like to thank my advisor, Dr. Robert S. Carmichael, for his advise and support during this work. He not only designed and supplied a good deal of the equipment used, but also furnished many of the ideas for this work.

Dr. Ted Vinson of the Civil Engineering Department supplied the hydraulic press and other items of support.

Dr. Jerry Cowen of the Physics Department loaned a digital voltmeter and integrator for the ballistic magnetometer.

I would like to extend special thanks to my colleague Joon Kim, who assisted in much of the experimental work, and frequently put up with my unorthodox working hours.

The figures were produced by Yvonne Plaisance and Jake Keeser of Chevron Oil Company.

APPLICATION OF A HIGH PRESSURE MICROBOMB TO HYDROSTATIC PRESSURIZATION OF MAGNETITE

A THESIS SUBMITTED TO THE DEPARTMENT OF GEOLOGY OF MICHIGAN STATE UNIVERSITY IN PARTIAL FULFILLMENT OF THE REQUIREMENTS FOR THE DEGREE OF MASTER OF SCIENCE

By
JOHN KELLY MAHER
JUNE, 1976

TABLE OF CONTENTS

List	of	Figu	res											
I.	Int	rodu	ction	•	•			•	•	•	•	•	•	-
II.	The	ory	•			•	•				•	•		3
	Α.	Dom	ain E	nerg	ies	•			•	•	•	•	•	3
		1.	Excha	ange	ene	rgy	•		•	•		•	•	4
		2.	Magne	etoci	ryst	alli	ne ar	niso	trop	y ene	ergy	•]
		3.	Domai	in wa	a11	ener	gy	•	•	•		•	•	6
		4.	Magne	etosi	tric	tive	anis	otr	ору	ener	gy	•	•	•
		5.	Magne	etosi	tati	c en	ergy	•	•	•	•	•	•	9
		6.	Field	l ene	ergy			•	•	•		•	•	9
	В.	Gra	in Si	ze Ei	ffec	ts	•	•	•	•	•	•	•	9
III.	Equipment and Experimental Techniques											•	14	
	Α.	Pre	vious	worl	ĸ	•	•		•	•	•	•	•	14
	В.	Pre	ssure	mici	roboi	mb	•		•	•	•	•	•	14
	С.	Ope	ration	ı	•	•	•	•	•	•		•	•	19
	D.	Ba1	listic	: Mag	gnet	omete	er		•	•	•	•	•	22
IV.	Sample Specifications and Experimental Results													29
	Α.	Gen	eral p	prope	erti	es o	f mag	gnet	ite	•		•	•	29
	В.	Sam	p1es	•	•	•		•	•	•		•	•	29
	С.	Mag	netic	resu	ults		•	•	•	•		•	•	30
V .	Int	erpr	etatio	on of	f Re	sult:	5	•	•	•	•	•	•	38
VI.	Con	c1us	ion	•		•		•	•	•			•	4 (
	App	endi	x A -	Bomb	Ca	libra	ation	n Da	ta	•		•		4 2
	Ribliography												43	

LIST OF FIGURES

I - 1	Possible domain structures	12
I - 2	Fringing field at a plane surface	12
I - 3	Variation in rotation with distance from domain wall center	13
II-1	Non-magnetic pressure chamber and ballistic magnetometer	15
II-2	Piston assemblies	18
II-3	,,	21
II-4	using NH ₄ F Hydraulic press force vs internal confining pressure inside bomb	23
II-5	Sense coil field	24
II-6	Mutual cancellation of solenoid and lab fields	26
II-7	Schematic diagram of equipment set-up	27
III-1	Magnetization vs pressure - sample 7	34
III-2	Magnetization vs pressure - sample PH-3	35
III-3	Magnetization vs pressure - sample PH-3	36
III-4	Magnetization vs pressure - sample PH-3	37

I. INTRODUCTION

To date, laboratory research on magnetic properties of earth materials under simulated crustal conditions has centered on high temperature experiments and tests involving application of uniaxial pressure. Little work has been done concerning properties of minerals and rocks under realistic high hydrostatic pressure. The latter can be an important factor in the behavior of physical parameters of rocks and minerals. For example, Stesky and Brace (1973) have shown that the electrical conductivity of oceanic basalts varies with increased confining pressure, and Carmichael (1969) has shown a variation of coercive force in magnetite with hydrostatic pressure. Breiner and Kovach (1966) used pressureinduced changes in magnetization of rock to try to forecast seismic events along the San Andreas fault. Other recent studies of applications of geopiezomagnetism to earthquake prediction include those by Golovkov (1969), Rikitake (1968) and Johnston (1975). Davis and Stacey (1971) noted that a local magnetic anomally was produced in the area of a dam, as a result of crustal loading when the reservoir was filled.

Since most crustal rocks are, or have been, subjected to confining (hydrostatic) pressures of at least several kilobars, it is important in the study of geopiezomagnetism to understand the effects of confining pressure on magnetic materials. Both transient and permanent effects of pressure need to be studied to understand the true nature of magnetic remanence in rocks, and how it changes in the lithosphere.

Specifically, this paper is intended to study the nature of the variation of the magnetization of magnetite within the pressure range of one atmosphere to five kilobars. Isothermal remanent magnetization was monitored as hydrostatic pressure on the magnetite samples was increased from one atmosphere to about three kilobars, then decreased to two kilobars, increased again to four kilobars and finally released to about one kilobar (the pressure held within the pressure bomb by the frictional force of the packing material). A significant drop was noticed in the magnetization with the first pressurization to two kilobars, J dropping to about 70% of the initial saturation. Little change in J was noticed beyond 2.0 kilobars.

The samples used were a magnetite crystal and a synthetic magnetite powder. The powder was mixed with a resin matrix to simulate a rock with a high magnetite content.

A fundamental part of this type of study is the development of technology capable of both simulating a high pressure environment and allowing for convenient measurement of the magnetic properties of the sample.

This work is intended to contribute something both to the technology of current high pressure experimentation and to the understanding of rock magnetism.

II. THEORY

Domain theory describes the magnetization of individual mineral grains; the magnetization of such grains in rock governs the magnetic behavior of the rock as a whole and is therefore of prime importance in the study of rock magnetism. The limit of how well the magnetic properties of minerals are understood is the limit to how well paleomagnetism may be understood and relied upon.

Grain size is a prime factor in the magnetization of mineral grains and as such is an important factor in how long a rock will hold its natural remanent magnetization, and to what extent changing conditions affect that remanence.

The effect of grain size may be better understood by viewing the energies involved in rock magnetization. Both the energies and sizes of grains are interrelated with the structure of domains within ferromagnetic mineral grains. A number of good reviews of the subject may be found in the literature (Neel, 1955; Stacey, 1963; Kittel, 1949, Chikazumi, 1964; Stacey and Banerjee, 1974).

DOMAIN ENERGIES

The purpose of domains in ferromagnetic minerals is to minimize the total magnetic energy of the particular specimen. Since ferrites possess spontaneous magnetization below the Curie temperature, magnetic fields will be set up within the material, and these will extend beyond the sample surface. This increases the magnetic energy of the specimen,

causing it to be in an unstable state--hence the formation of domains. The total magnetic energy of a ferrite grain may be divided into six components, which will be briefly described.

- 1. Exchange Energy, $E_{\rm X}$. This is produced by the interaction of electron spins of adjacent atoms, and was derived initially by Heisenberg. This energy can be minimized when the magnetic moments of adjacent spins are parallel. If a domain wall between two antiparallel domains is considered to be of infinitessimal thickness, then the angle between the spin axes will be 180° , with a maximum exchange energy. But by making the domain wall relatively thick, with many contained spin axes, then the angle between any two spin axes can be reduced, thus reducing the exchange energy density.
- 2. Magnetocrystalline Anisotropy Energy, E_k . Sometimes called the anisotropy energy or crystal magnetic anisotropy energy (Chikazumi, 1964), this energy is a measure of the preference of a ferromagnetic crystal for spontaneous magnetization along particular crystallographic axes (Kittel, 1949; Chikazumi, 1964). The direction of preferred magnetization is called the direction of "easy" magnetization; the most difficult directions are called the hard directions. The excess energy required to magnetize a grain in the hard direction, as opposed to the easy direction, is the anisotropy energy, E_k (Kittel, 1949).

Expressions for E_k , in terms of the direction cosines of the internal magnetization, have been worked out in most discussions (Chikazumi, 1964; Kittel, 1949; Stacey, 1963). For a cubic crystal system, two anisotropy constants are used, K_1 and K_2 ; the value of E_k for a cubic crystal, such as given below (α_1 , α_2 , α_3 are the direction cosines of the magnetization vector with respect to the three cube edges):

(1)
$$E_k = K_0 + K_1 (\alpha_1^2 \alpha_2^2 + \alpha_2^2 \alpha_3^2 + \alpha_3^2 \alpha_1^2) + K_2 \alpha_1^2 \alpha_2^2 \alpha_3^2$$

Both anisotropy constants are temperature-dependent, and can vary enough to change sign of the net E_k . K_1 is generally more important than K_2 (Stacey, 1963).

In magnetite, the easy axes are the <111> axes, and the anisotropy constants are negative, so we are primarily concerned with a magnetization inclined at some angle Θ to the <111> axis. To a second-order function in $\sin \Theta$ (Stacey and Banerjee, 1974) the above equation reduces to

$$E_k = (\frac{K_1}{3} + \frac{K_2}{27}) - (\frac{2K_1}{3} + \frac{2K_2}{9}) \sin^2 \Theta,$$

the second term dropping out as the magnetization aligns itself with the easy axis. For pure magnetite at 290° K, $K_1 = -1.36 \times 10^5$ ergs/cc and $K_2 = -0.44 \times 10^5$ ergs/cc, making E_k , at -1.80×10^5 ergs/cc, lowest along <111>.

A more gradual rotation of spins in domain walls, while decreasing the exchange energy, increases \mathbf{E}_k by forcing some spins out of the easy direction of magnetization. However, while $\mathbf{E}_{\mathbf{x}}$ is affected by this movement of spins within the

crystal, the exchange energy itself does not produce any anisotropic effects. The origin of magnetocrystalline anisotropy is due rather to atomic interactions: "the spin interacts with the orbital motion (of the electrons) by means of the spin-orbit coupling and the orbital motion in turn interacts with the crystal structure by means of the electrostatic fields and overlapping wave functions associated with neighboring atoms in the lattice" (Kittel, 1949).

- 3. Domain Wall Energy, E_w . This is a function of the minimized sum of the exchange and anisotropy energies $(E_x + E_k)$. In a uniaxial model the exchange energy per unit area of wall is given by
 - (2) $E_{\chi} = \int A(\delta \Phi / \delta \times)^2 d \times$ (Craik and Tebble, 1965)

where A is the exchange constant and Φ is the angle of spin rotation as a function of x (see Fig. I-3). In the same model, E_k per unit area is given by

(3)
$$E_k = \int K_1 \sin^2(\Phi) dx$$

where K is the anisotropy coefficient. The energy of the wall using the above values for $\rm E_x$ and $\rm E_k$ is then given by

(4)
$$E_w = 2 (AK_1)^{\frac{1}{2}}$$
 (Stacey, 1963)

this being approximately 1 erg/cm^2 , while letting A equal the exchange energy for spin S and lattice spacing "a" -- A = J is the exchange integral.

4. Magnetostrictive Anisotropy Energy, $E_{\lambda\sigma}$. When a crystal is stressed, the domains and walls within it are physically moved. This movement causes subsequent changes in the directions of the domain magnetization vectors, and a change in the net magnetization of the crystal. The energy associated with this change in magnetization is the magnetostrictive anisotropy energy (also referred to as the magnetoelastic energy or the magnetostrictive strain energy). $E_{\lambda\sigma}$ is defined to be zero for an unstrained lattice (Kittel, 1949). It should be kept clear that when the magnetization induces a physical change in the shape of a specimen the effect is termed magnetostriction; when applied stress on the specimen induces a change in magnetization, the effect is termed inverse magnetostriction, or piezomagnetism.

When a ferromagnetic body is placed in a magnetic field, interaction between the atomic magnetic moments causes a change in bond lengths, since $E_{\lambda\sigma}$ is a function of the interatomic distance \underline{r} . For a cubic lattice, $E_{\lambda\sigma}$ may be expressed in terms of the lattice strain tensor components (e_{ij}) and the direction cosines of the domain magnetization (a_i) as (Chikazumi, 1964) for the one-dimensional case:

(5)
$$E_{\lambda\sigma} = B_1 \left(e_{xx}(a - 1/3) + e_{yy}(a - 1/3) + e_{zz}(a - 1/3) \right)$$

 $+ B_2 (e_{xy}a_1a_2 + e_{yz}a_2a_3 + e_{zx}a_3a_1)$
where $B_1 = N(\frac{dL}{dr})r_0$, $B_2 = 2NL$

and N = demagnetization factor, L = specimen length.

If a stress σ is applied to a ferromagnetic material, the energy due to that stress may be expressed by giving the strain tensor components of the magnetoelastic energy in terms of the direction cosines g_i , the stress, and the elastic constants s_{ij} : as,

(6)
$$e_{xx} = \sigma(s_{11}g_1^2 + s_{12}(g_2^2 + g_3^2))...$$

By substituting (6) and (5), we arrive at a new expression for $E_{\lambda\sigma}$:

(7)
$$E_{\lambda\sigma} = B_1 \sigma (s_{11} - s_{12}) (a_1^2 g_1^2 + a_2^2 a_2^2 + a_3^2 g_3^2 - 1/3)$$

+ $B_2 \sigma s_{44} (a_1 a_2 g_1 g_2 + a_2 a_3 g_2 g_3 + a_3 a_1 g_3 g_1)$

If, for example, the magnetization of the domain is parallel to the (111) face, $E_{\lambda\sigma}$ may be expressed in terms of 0, the angle between the direction of tension in the crystal and the (111) face:

(8)
$$\cos(\Theta) = (1/3)^2 (g_1 + g_2 + g_3)$$
 and

(9)
$$E_{\lambda\sigma} = +\frac{3}{2} \lambda_{111} \sigma \cos^2(\Theta)$$

The same holds for other domain directions, with the substitution of the correct value for λ , the saturation magnetization strain (Chikazumi, 1964).

The dependence of the magnetostrictive energy on the domain configuration becomes complex in the three-dimensional real case. However, a two-dimensional example computed for

the four domain case of Fig. I-1.c (Stacey and Banerjee, 1974) serves to give an order of magnitude value for $E_{\lambda\sigma}$ in magnetite of 6 x 10³ ergs/cc, compared to -2 x 10⁵ ergs/cc for E_{k} .

- 5. Magnetostatic Energy, E_m . When free poles exist at the surface of a grain, they give rise to the magnetostatic energy, given by
- (10) $E_m = \frac{1}{2}NJ_S^2$ (for an ellipsoid) (Stacey, 1963) where J_S is the saturation magnetization parallel to the long axis of the ellipsoid and N is the demagnetization factor. The strength of E_m is dependent upon the shape of the sample and the number and strength of free surface poles.
- 6. Field Energy, E_h . A grain may also acquire a field energy when in a magnetic field \underline{H} , with magnetization \underline{J} of the sample. The energy per unit volume is given as
- (11) E_h = HJ cos0 (0 = angle between J & H) (Stacey, 1963). This may cause the enlargement of domains oriented in the general direction of \underline{H} , while opposing domains will be reduced.

GRAIN SIZE EFFECTS

The importance of grain size in the study of domains is evidenced by the several properties dependent upon it: such properties include coercive sorce, susceptibility, and transitions from the superparamagnetic state to single domain and multidomain states.

Consider first a spherical isotropic grain of sufficient size to contain only one domain. The energy of the grain is then given by the magnetostatic energy only (Nagata, 1961):

(12)
$$E_m = \frac{1}{2}NJ_s^2(4/3)\pi R^3$$
, where $N = \pi^2 4/3$.

As grain size increases, a point is reached where the inclusion of a domain wall will decrease the energy of the grain, by decreasing the magnetostatic energy by a greater amount than is gained by the addition of the wall energy. The new grain energy is given by the sum of $E_{\rm w}$ and $E_{\rm m}$, the new total energy now being reduced by 50%:

(13)
$$E_{\text{total}} = \frac{1}{2} (\frac{1}{2} J_s^2 R^3) (4\pi/3)^2 + \pi R^2 \alpha_w$$

where $\alpha_{_{\boldsymbol{W}}}$ is the wall energy per unit area.

The theoretical critical radius, R_2 , may be found by equating the total energies of the single and multidomain states. In this instance, the value for R_2 is (Nagata, 1961)

(14)
$$R_2 = 9\alpha_w/4\pi J_s^2$$
.

Single domain particles range in size from 0.1 microns in diameter to 0.5 microns. From 0.5 to 20.0 microns grains undergo a transition from the single domain state to the multidomain state. Grains in this range are termed pseudosingle domain particles. Grains larger than 20.0 microns are multidomain only. (These values are for magnitite).

Single domain particles have coercive forces that are greater than either SPM or MD particles. Neel (1955) states

that this occurs because wall displacements, necessary in the movement of a multidomain particle through the hysteresis cycle, require a release of energy, while this is not a factor with single domain grains. SPM particles have smaller values of H_c because below a certain volume, \underline{v} , the thermal agitation energy kT becomes large with respect to the energy terms dependent upon \underline{v} and the anisotropy constant \underline{K} , such that kT exceeds $\underline{K}\underline{v}$ $\sin^2(\Theta)$. This perturbs the precession of the atomic moments, altering Θ and causing the remanence to decay with time, according to J_r - $J_O \exp(-t/t_O)$, t_O being the relaxation time (Neel, 1955).

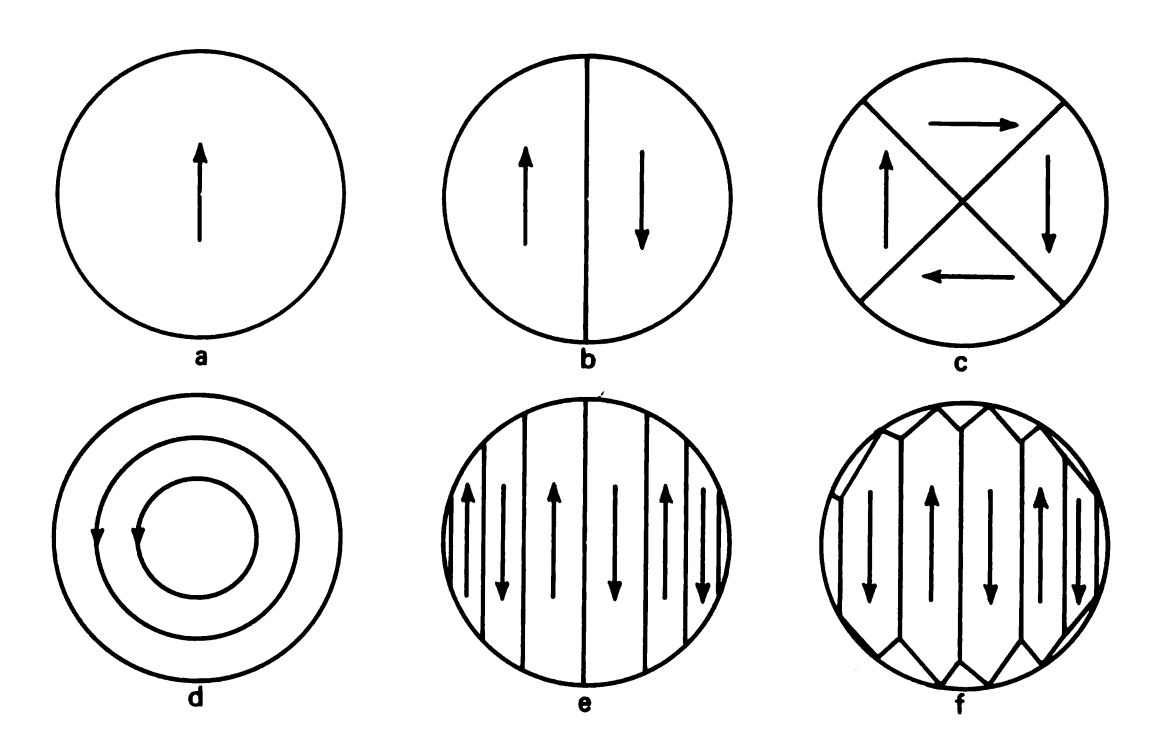


FIGURE I-1

POSSIBLE DOMAIN STRUCTURES (After Stacey, 1963)

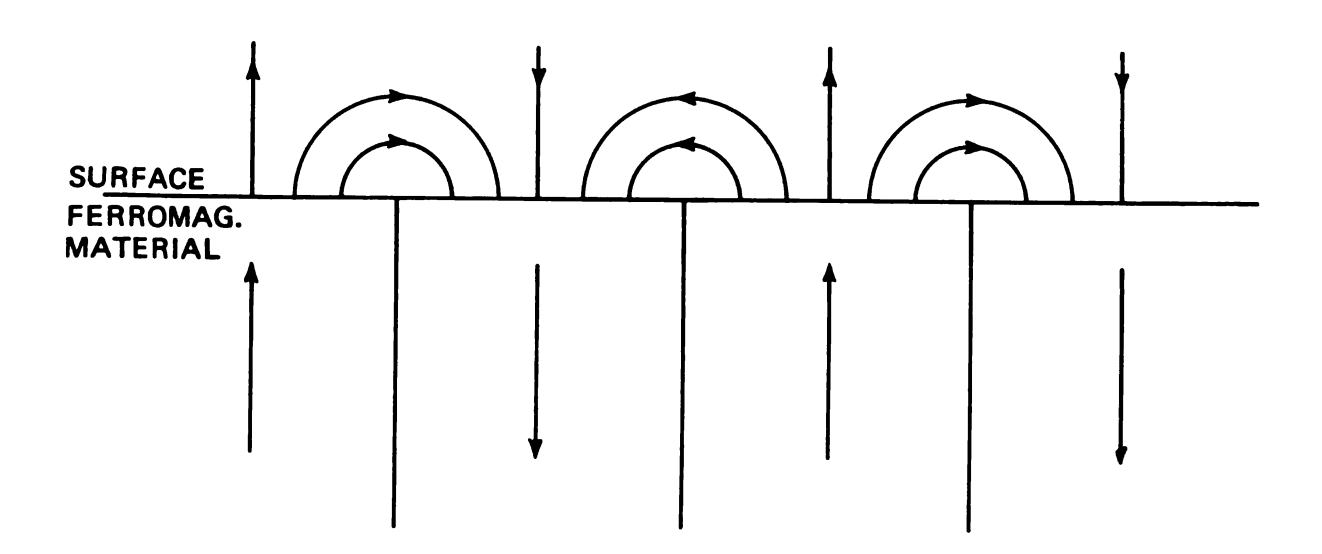


FIGURE I-2
FRINGING FIELD AT A PLANE SURFACE (After Stacey, 1963)

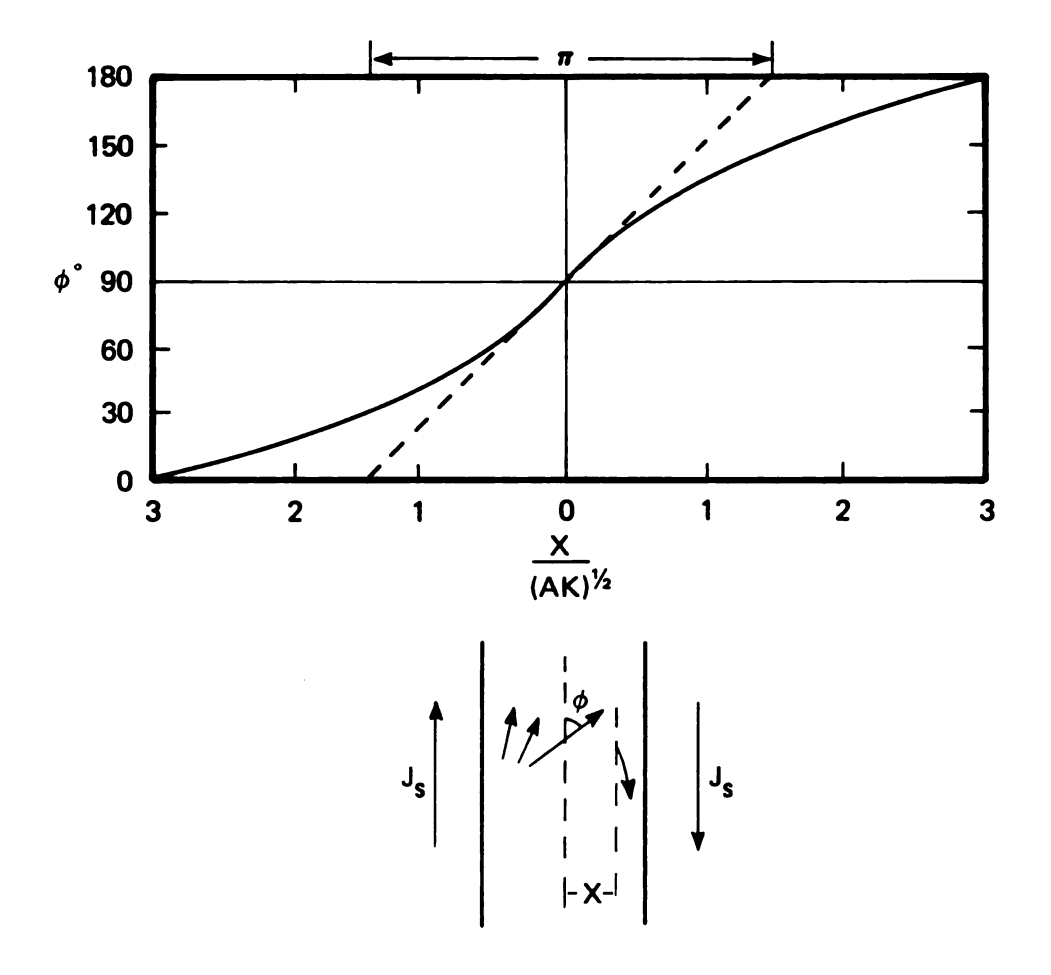


FIGURE I-3

ABOVE IS THE VARIATION IN ROTATION WITH DISTANCE FROM THE DOMAIN WALL CENTER.

BELOW IS THE MAGNETIZATION DIRECTION WITHIN THE DOMAIN WALL. (After Craik and Tebble).

III. EQUIPMENT AND EXPERIMENTAL TECHNIQUES

A large part of this study involved the development of new high-pressure apparatus and subsequent modifications of this equipment. The following is a discussion of the equipment and techniques used.

PREVIOUS WORK

The study of geophysical properties of earth materials under hydrostatic pressure has previously been largely restricted to the pressure range of less than two kilobars, with the exception of some velocity studies and some work in electrical conductivity (Stesky and Brace, 1973). Experiments in solid-state physics have gone into hundreds of kilobars, but these studies usually begin at approximately 10 kilobars, and are not done on earth materials. The purpose of the present study is to partially fill the 2--10 Kb gap.

Until recently, research into the magnetic properties of minerals has generally been restricted to tests under uniaxial pressures. However, effects of high hydrostatic pressure on the Curie temperature of magnetite (Schult, 1970), and on coercive force and saturation remanence (Carmichael, 1969) have been observed.

PRESSURE MICROBOMB

The pressure vessel used in this study is essentially that described in previous studies (Carmichael, et al, 1968). It is a piston apparatus (Fig. II-1) of beryllium copper

NON-MAGNETIC PRESSURE CHAMBER AND BALLISTIC MAGNETOMETER

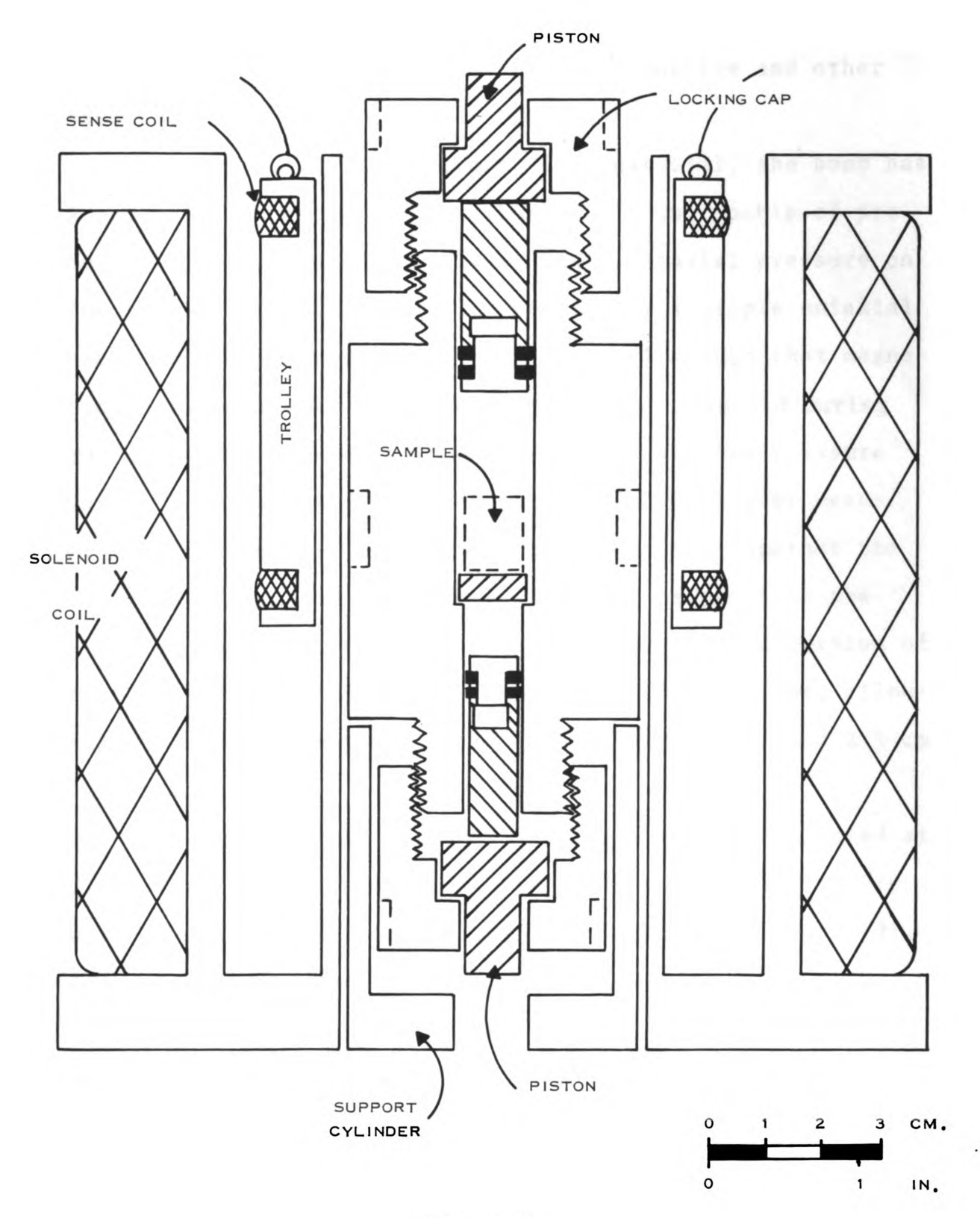


FIG. II-1

alloy (1.81% B_e by weight) and is capable of sustaining internal pressures to 11 kilobars. The bomb is diamagnetic, with a susceptibility of -0.6×10^{-7} emu/gm at 20° C, so magnetic changes due to the bomb with variations in applied fields are negligible compared to changes in magnetite and other samples.

Aside from its non-ferromagnetic material, the bomb has a number of other unique attributes. It is capable of producing both hydrostatic pressure and a uniaxial pressure on the sample simultaneously, and needs only a simple uniaxial press to achieve this. The bomb is small enough that magnetic measurements may be made with a small solenoid during pressurization, and it is easily portable. The pressure may be held in the bomb for long periods of time by means of the locking caps, which may be screwed down against the mushroom pistons on either end, thus making possible the study of long-term pressure effects. The present version of the bomb has a larger sample space than the original, allowing the study of samples up to 1.2 cm in diameter and 2.5 cm in length.

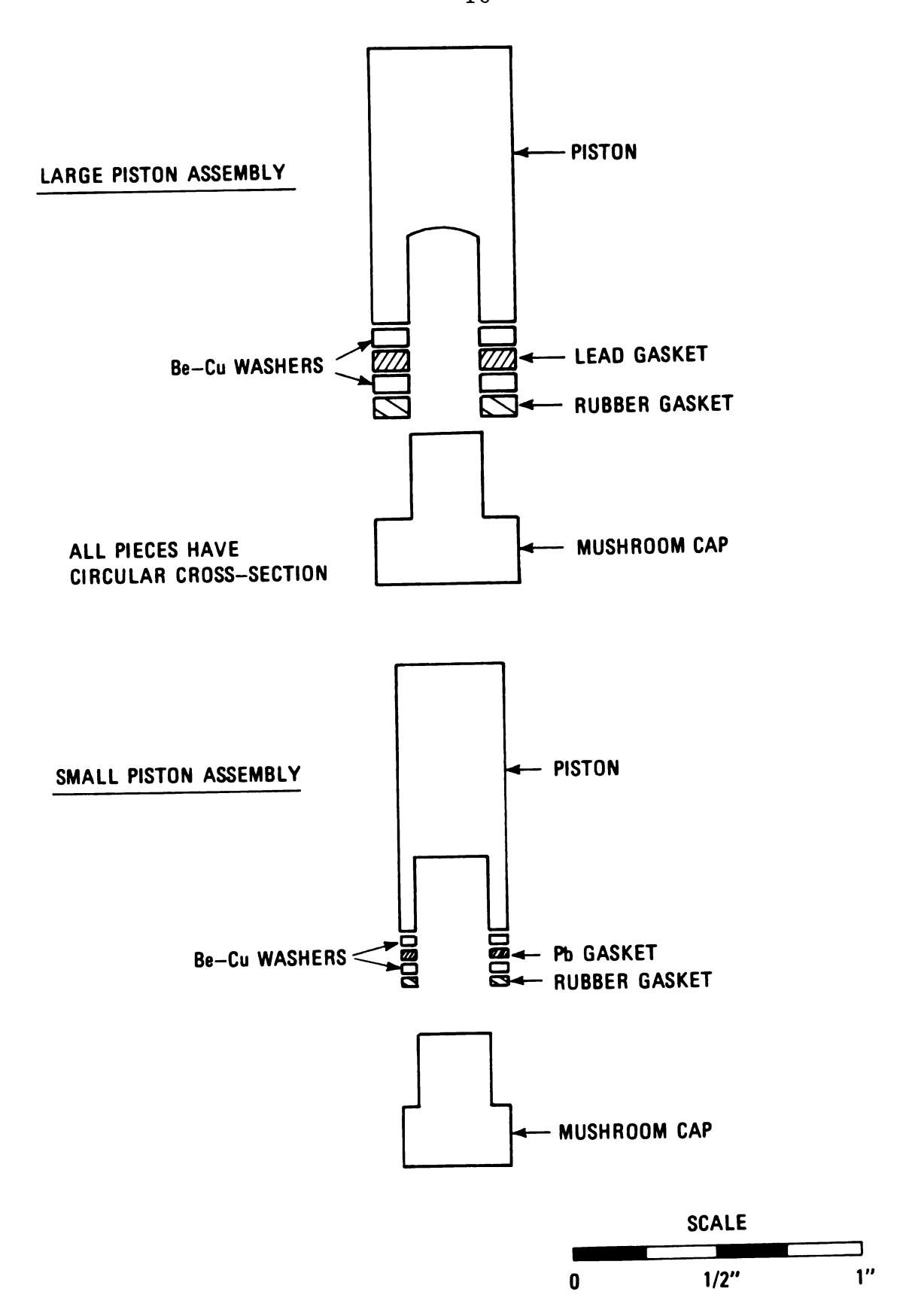
After machining, the bomb used here was heat treated at 316°C for four hours. After heat treating, the parts were work hardened by the method outlined by Paul, et al (1959). All materials were work hardened up to 5.5 Kb.

Following several pressure runs to four kilobars, the large piston's mushroom cap sheared around the base. The outer ring of the cap had been supported by the washers and

shoulder of the main piston, while the inner portion of the cap was forced down into the recess in the outer piston by the confining pressure (see Fig. II-2). This was corrected by modifying the piston and cap: the flanged ends of each cap were increased in thickness, and the length of the neck of the cap was increased.

The modification corrected the problem with the mushroom caps, but the stress previously absorbed by the caps was now transferred to the shoulders of the main pistons. No ill effects were noted at pressures below four kilobars, but at pressures between 4.0 and 5.5 kilobars the main piston of the large piston assembly began to deform, expanding the portion of the piston between 0.2 and 0.5 centimeters below the bottom of the recess. This expansion made removal of the piston assembly difficult, and greatly increased the friction between the cylinder wall and the piston during pressure runs, thereby adding an uncertainty in the value of the internal confining pressure with increasing applied press force. The piston was remachined to its original diameter, but this weakened it enough to cause shearing in the previously expanded area.

The large piston was again modified, this time by reducing the diameter of the recess and corresponding neck of the mushroom cap. This allowed the stress to be absorbed by a greater area of the piston, and to be concentrated more toward the center of the piston instead of at its perimeter. The final versions of the pistons are shown in Figure II-2.



PISTON ASSEMBLIES

FIG. 11-2

One final modification of the previous bomb was made.

When extracting the pistons and sample from the bomb after pressurization, a force of several hundred pounds is required to drive out the large piston. Single crystal samples generally cannot sustain such large directed stress without crushing. To prevent destroying the samples after each pressurization, a brass bushing was made to fit around the sample. Thus, when the large piston is driven out by forcing the small piston through the entire length of the bomb, this force is absorbed by the bushing and not the sample. Small notches were filed in each of the bushings to allow free fluid flow around the sample during pressurization.

OPERATION

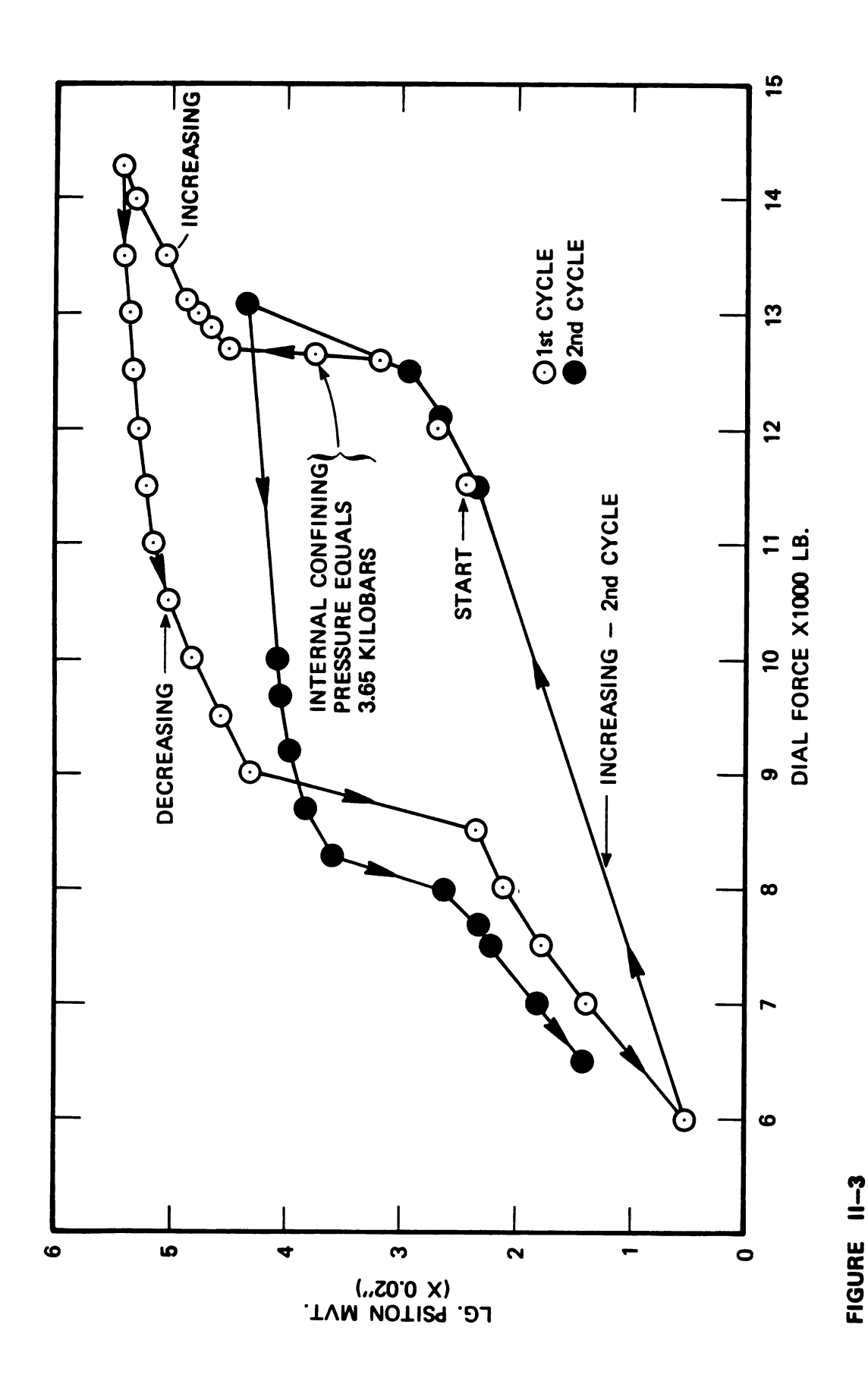
Pressurizing techniques for the current research closely followed tyose outlined for the original bomb (Carmichael, et al, 1968). A fluid pressure-transmitting medium of a 1:1 mixture of kerosene and transformer oil was used. A fluid pressure medium makes for more difficult sealing, but some advantages are gained over solid pressure-transmitting mediums: uniform confining pressure is assured, so there is no concern about possible pressure gradients (Paul, et al, 1959) and though the oil mixture congeals at low temperature, there is a low fractional change in volume and therefore little hydrostatic pressure loss (Carmichael, et al, 1968).

The sample was first coated with resin to prevent oil from entering any small cracks and causing the sample to disintegrate under pressure. The sample was then glued to

the base plate and inserted into the microbomb. One piston was then driven into the cylinder far enough to allow the corresponding locking cap to be secured. The chamber was then filled with oil, the other piston enserted and the second locking cap secured.

Seals around the pistons were provided by two gaskets, one of rubber and one of lead. The rubber gasket expands against the wall of the cylinder upon slight pressurization, and may be tightened by hand to a sufficient degree to prevent leakage. As pressure is applied by a press, the lead gasket is compressed between the two Be-Cu washers, flowing out around the piston to form a seal sufficient to withstand the pressures involved (Fig. II-2).

Internal hydrostatic pressure was determined using a sample of NH₄F. This crystal undergoes a change of phase at 3.65 Kb, and reduces in volume by about 30%. The sample of NH₄F was sealed by an impermeable rubber membrane, and piston displacement was monitored versus applied press pressure. A typical calibration curve of several tests for this microbomb is given in Figure II-3. The sudden change in the slope of the curve indicates the point where internal pressure has reached 3.65 Kb; the sample has suddenly reduced its volume, and the pistons have moved in rapidly to maintain a constant pressure. The half-width of the hysteresis loop of each pressure cycle is approximately equal to the packing friction between the large piston and the cylinder wall (Paul, et al, 1959). Internal hydrostatic pressure is assumed to be a

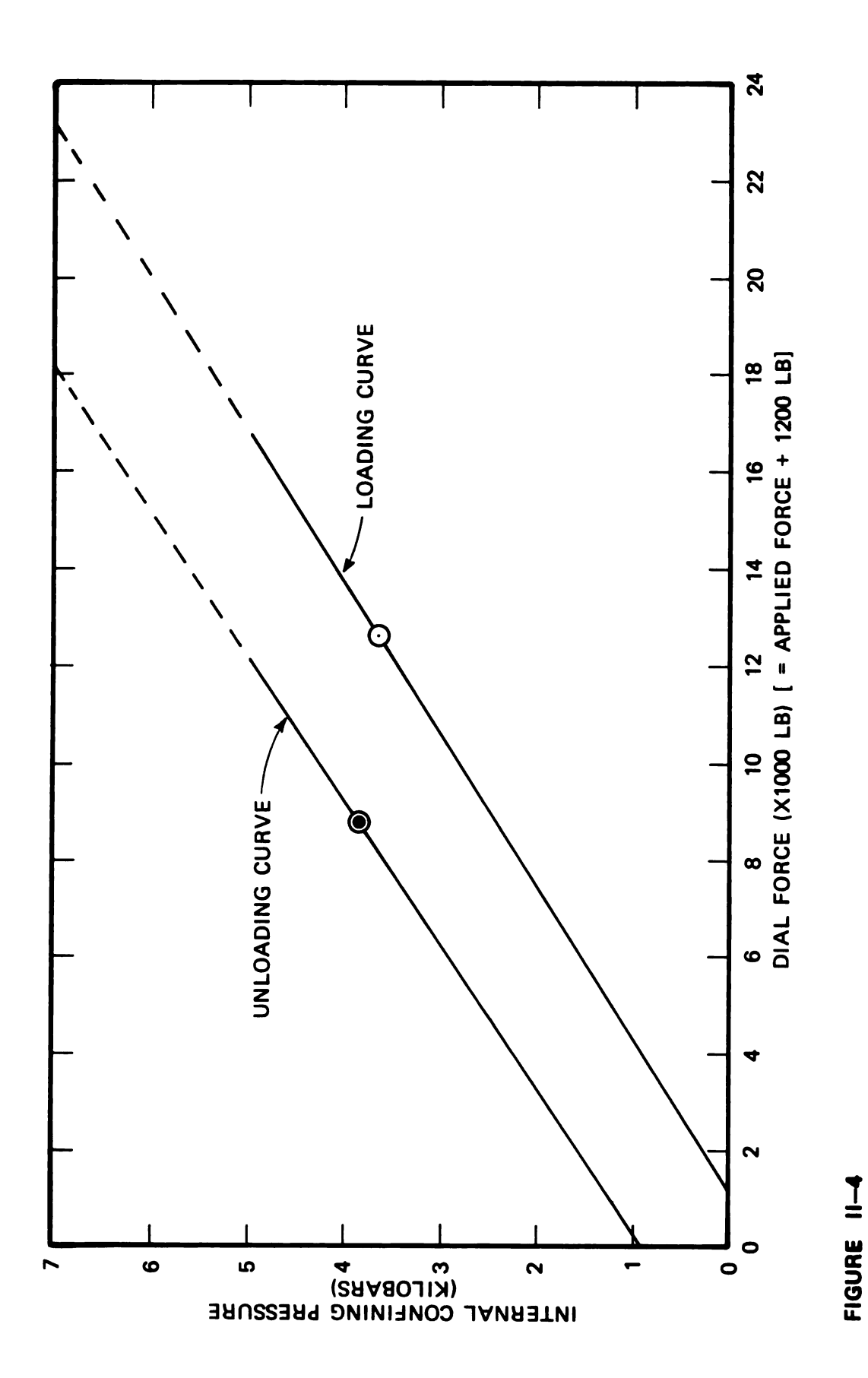


A TYPICAL CALIBRATION OF PRESSURE MICROBOMB USING NH4F

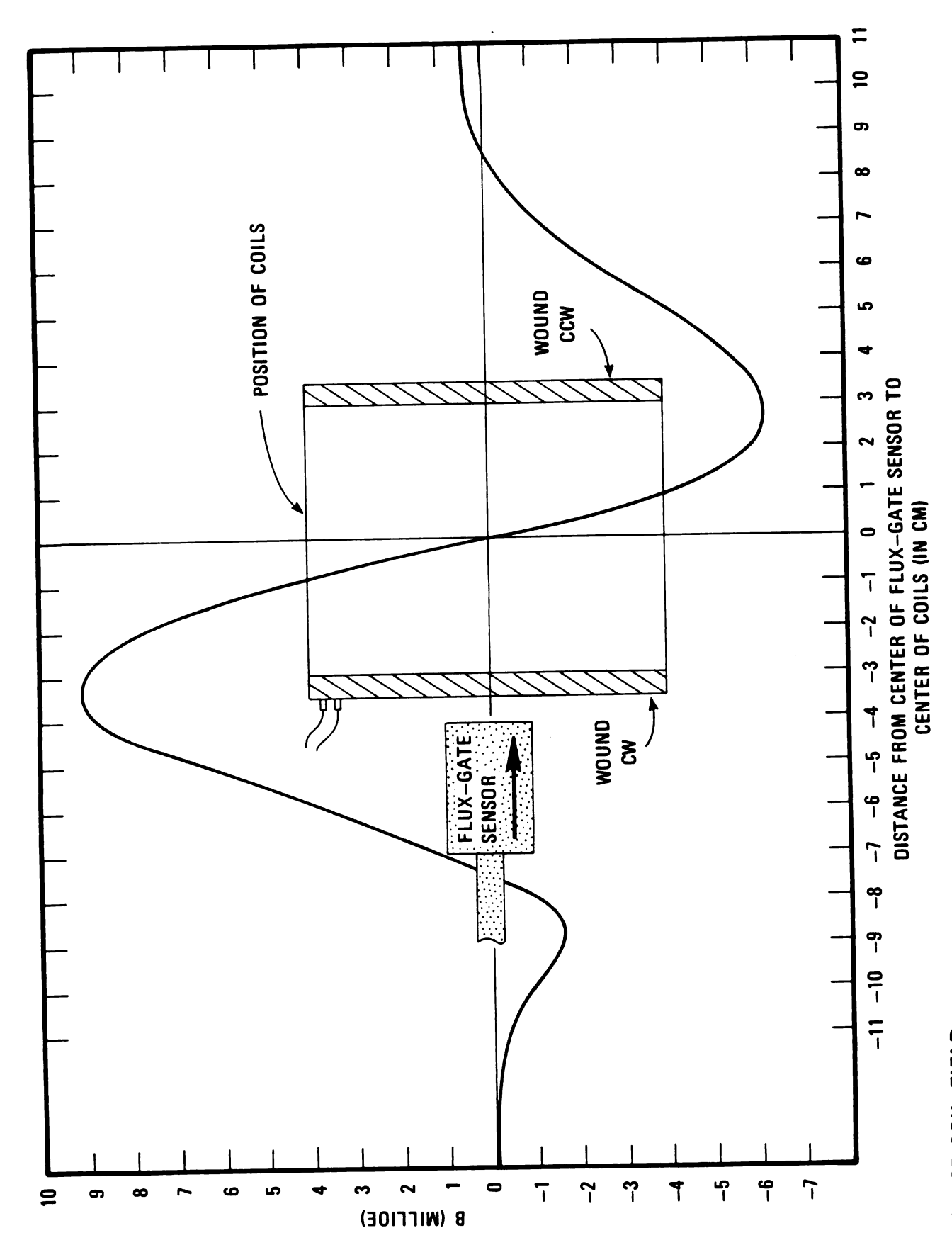
linear function of the applied pressure on the piston(s), and a plot of internal hydrostatic pressure versus applied force is given in Figure II-4. Applied force in Figures II-3 and II-4 is accurate to within 100 pounds. This implies that the hydrostatic pressure is accurate to ± 0.1 Kb.

BALLISTIC MAGNETOMETER

Measurements of magnetic properties involved the use of a ballistic magnetometer, consisting of a solenoid, a pair of sense coils (coil A wound in the opposite direction from coil B), a D-C power supply, and an integrator and a digital voltmeter (DVM). The ambient lab field inhomogeneities may be either nulled out by the solenoid, or a large field (30 to 60 gauss) may be produced. By moving the sense coils up and down within the solenoid (see Figure II-1), changes in magnetic flux within the solenoid induce electrical current changes within the coils. These changes in current are transmitted through the integrator and read as a total voltage change on the DVM. Thus, a change in total magnetic flux from the bottom to the top of the solenoid is read as a relative change in voltage. When a magnetic sample, such as magnetite, is introduced into the center of the solenoid, the flux lines are concentrated around the sample. Since the coils are wound oppositely, a maximum signal is obtained when the sample is effectively moved from one coil to the other. A sample curve of the field produced by a small current in the sense coils is shown in Figure II-5.



HYDRAULIC PRESS FORCE VS.
INTERNAL CONFINING PRESSURE INSIDE BOMB



5-11 513

SENSE COIL FIELD (WITH CURRENT OF 45 μΑΜΡS

The lab field within the press contained a small inhomogeneity. This could be either cancelled or strengthened
by the solenoid field, since the solenoid field was strongest
at the center, and the strength of the field dropped sharply
toward the ends of the coil. An example of the solenoid
field cancelling the lab field is shown in Figure II-6.

The equipment set-up used is shown schematically in Fugure II-7. The bomb, with sample, was placed in the center of the solenoid, which was positioned in the center of the hydraulic press, and the sense coil was manually moved vertically within the solenoid. Voltage changes were noted on the DVM.

The samples were first saturated in a 2 kilogauss field, and their initial saturation magnetization measured in a nulled field outside of the press before loading in the bomb. The field within the press was then checked to determine if the ambient field was nulled out by the solenoid field. This being done, the bomb, with sample, was placed within the coil, and the magnetization of the sample was measured in the press at one atmosphere. The sample was then pressurized, and readings of magnetization were taken at intervals of 0.5 Kb.

After cycling the pressure, a measurement of magnetization was made with no press pressure, leaving the sample under only the pressure due to the friction of the packing in the bomb (approximately 1.0 Kb). Final measurements were made with all pressure released, but with the sample and bomb still in the press, and outside the press and bomb. Magnetic data values are accurate to within $\pm 4.0\%$ of $J_{r,sat}$.

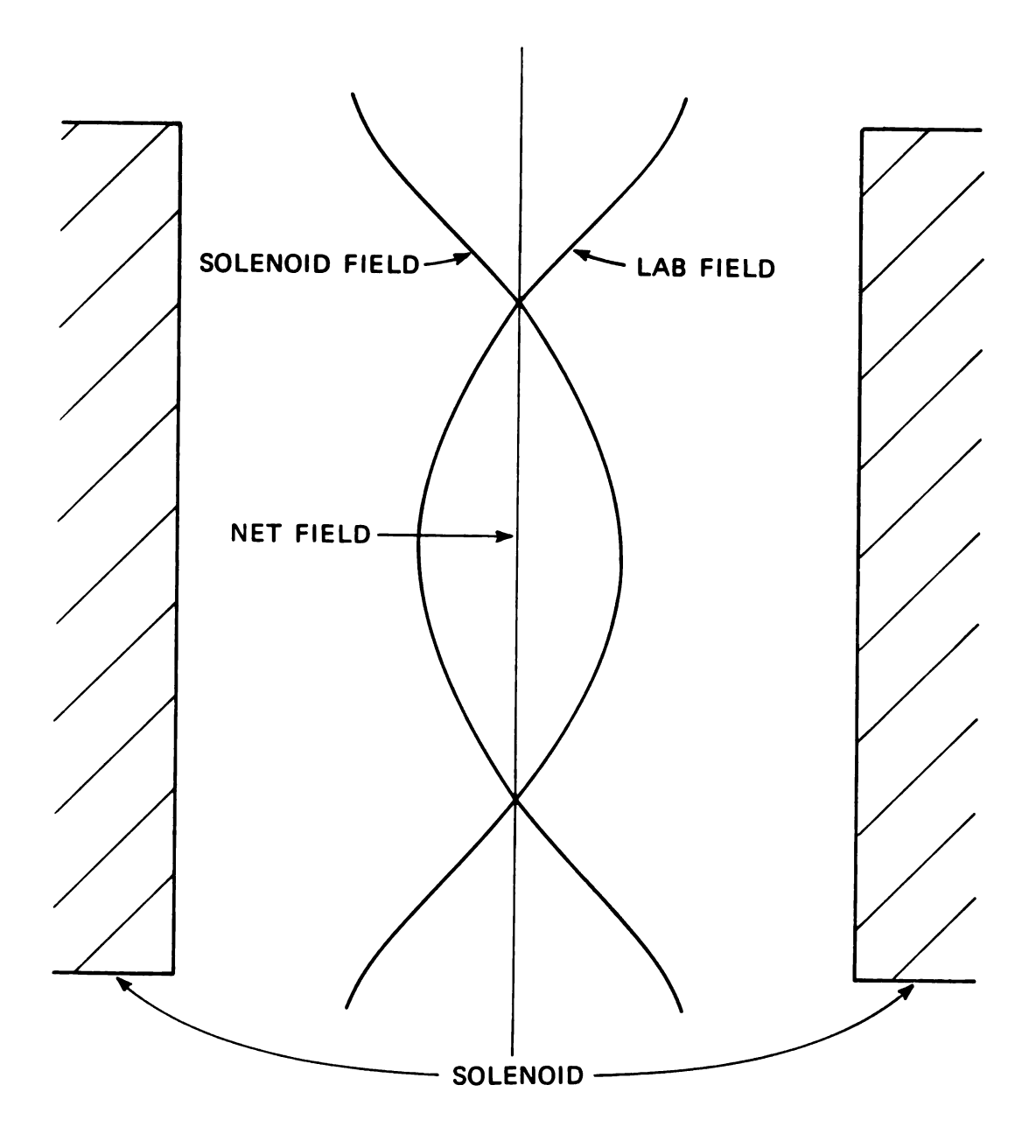


FIGURE II-6
MUTUAL CANCELLATION OF SOLENOID
AND LAB FIELDS

SCHEMATIC DIAGRAM OF EQUIPMENT SET-UP

It should be noted that absolute magnetization was not measured during pressurization. Relative changes in magnetization, J, were measured, and all plots of data give relative changes in the normalized magnetization, since the voltage changes registered on the DVM are directly proportional to magnetization changes $(J/J_0 = dV/dV_0)$.

IV. SAMPLE SPECIFICATIONS AND EXPERIMENTAL RESULTS

Two types of magnetite samples were used in the present work: a single crystal, and a synthetic "rock" composed of magnetite powder cemented in a resin matrix. A description of the samples is given below, followed by the magnetic results obtained.

GENERAL PROPERTIES OF MAGNETITE

Magnetite, $\mathrm{Fe_3O_4}$, is one of the most widespread of the oxide minerals. It is found in igneous bodies, contact-metamorphic deposits, as replacement deposits, some high-temperature sulfide veins, and in detrital beach deposits. It is a major ore mineral for iron; specimens showing strong natural polarity are called lodestone.

The magnetite unit cell is of cubic, inverse spinel structure. The mineral has no cleavage, but will show parting along the (111) faces.

It is ferrimagnetic at room temperature, and has a saturation magnetization of 92-93 emu/gm (Clark, 1966) hold radius from the single domain to multidomain state is 0.57 to 0.72 microns (Soffel, 1971; Dunlop, 1972). Other parameters are given in Table 1.

SAMPLES

The single crystal sample used was a magnetite rod, cored perpendicular to the (111) face. It is denoted as "Sample PH-3." Specifications are given in Table 1. The sample was

coated with an epoxy glue prior to any pressurization, to prevent the fluid from seeping into any cracks and damaging the crystal.

The magnetite used in the synthetic sample was a synthetic magnetite powder derived from an aniline chemical process. It had been previously roasted at 90°C to remove water, then it was ground and sieved to remove particles with diameters greater than 149 microns. Most particles were about 6 microns in diameter.

The grains were mixed into a resin compound at a ratio of one part magnetite to three parts resin. This mixture was poured into a plastic tube, allowed to harden, then cut into sections one centimeter in length.

Both samples (PH-3 and No. 7) were saturated in a 2 kilogauss field before any measurements were made. This produces a saturation isothermal remanence, $J_{r,sat}$.

MAGNETIC RESULTS

Results of pressurized tests within the solenoid are presented in Figures III-1 through III-4. Samples were pressurized to 3.0 kilobars initially, resulting in a magnetization drop to around 70% of the initial saturation magnetization. Pressure was then reduced to 1.5 kilobars, while noting a slight drop in magnetization of 2 to 3% $J_{r,sat}$. Then pressure was increased to 4.0 kilobars, causing another 2-3% decrease in J. The final reduction in pressure from the 4.0 Kb maximum to standard pressure showed the magnetization

to remain at the 4.0 Kb value to about 500 bars, at which point the magnetization increased by about 5%. The point of interest here is not so much the exact pressures at which J decreases or increases, but rather the trend of the samples to decrease with initial pressurization and then to stabilize somewhat during increasing stress.

The effect of the packing friction within the bomb should be noted here. Once pressurized to over 2.0 Kb, the frictional force of the lead packing worked to hold in approximately 1.0 Kb. This is shown by the two pressure curves of Figure II-4. As a result, less press force was needed on a decompression cycle than on a compression cycle to achieve a given internal pressure.

The factors most notably prone to error in measurement were press force and J. Press force oscillations on the order of 100. 1b. were noted on all tests, apparently as a result of the developed inertia, causing the press mass to continue moving. Since the magnetic affects of interest occurred at press forces of approximately 4,000 to 14,000 pounds, an allowable upper limit of percent error in applied pressure is $\pm 2.5\%$. These oscillations were probably damped out to some degree by the packing friction of the bomb.

Relative values of J were read as emf output in microvolts from the magnetometer. A single movement of the sense coil past a typical unpressured sample produced a voltage change on the order to 100. microvolts. Each measurement

was made three times, and the average value recorded. Values were reproducible to within 4. microvolts, or 4.0% of $J_{\rm r}$, sat.

Properties of Magnetite (Fe304)

98 emu/gm at 0° K Saturation magnetization (J_s) 92 emu/gm at 20° C Single domain -- MD critical diameter 0.5 - 20. microns $-1.36 \times 10^5 \text{ ergs/cc}$ K_1 , at $17^{\circ}C$ K_2 , at $17^{\circ}C$ $-0.44 \times 10^5 \text{ ergs/cc}$ 575°C Curie temperature, T $20 \times 10^{-6} \text{ cm/cm}$ λ_{100} $60 \times 10^{-6} \text{ cm/cm}$ λ_{110} $78 \times 10^{-6} \text{ cm/cm}$ λη 1 1 (from Carmichael, 1971; Stacey + Banerjee, 1974;) (Soffel, 1971; Dunlop, 1972)

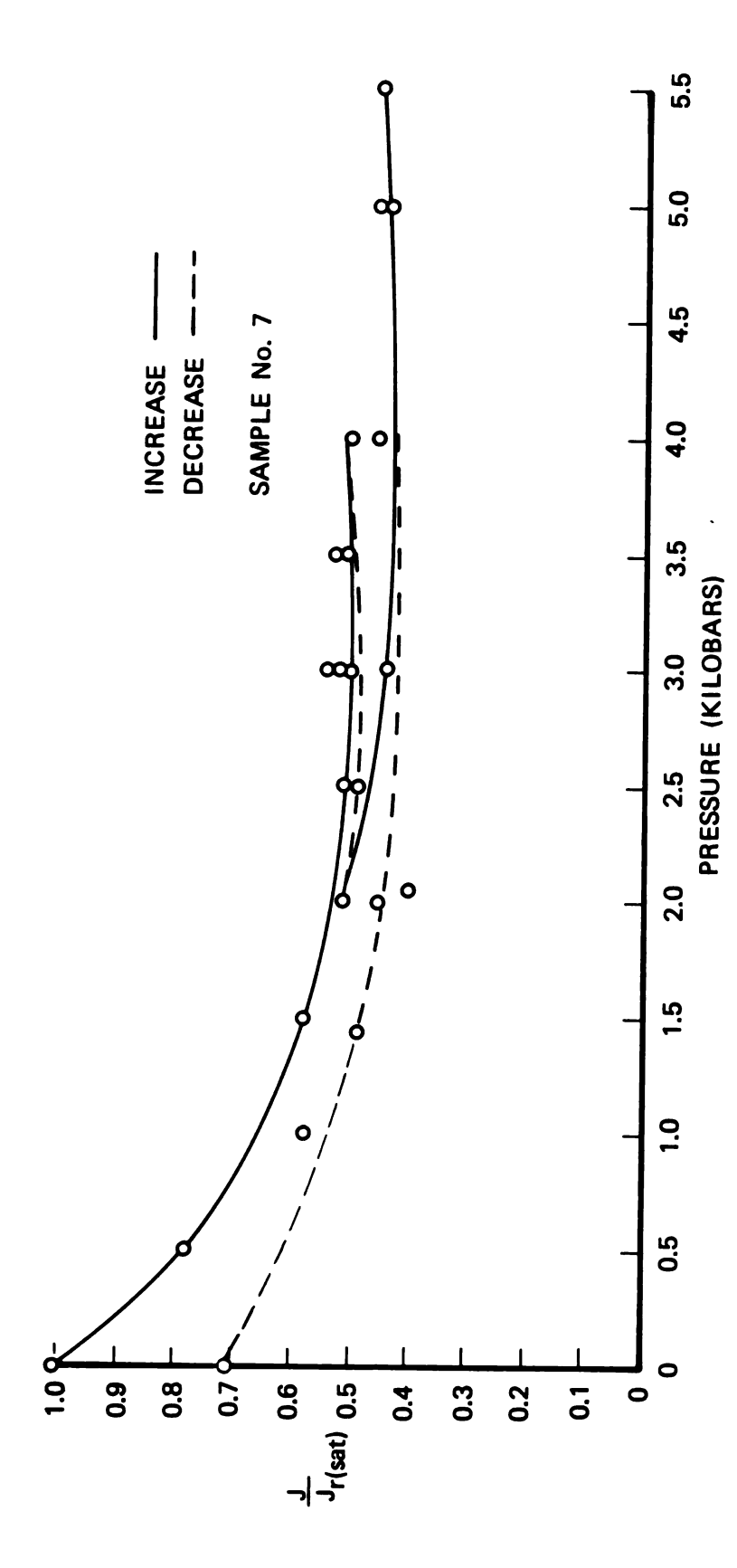
Sample PH-3

Sample 7 -- Magnetite powder

Synthetic Fe₃O₄; from aniline chemical process Average particle size grouped around 6 microns; 90% of particles between 1.5 microns and 20 microns. Very small trace amounts of Si, Al (Carmichael, 1975)

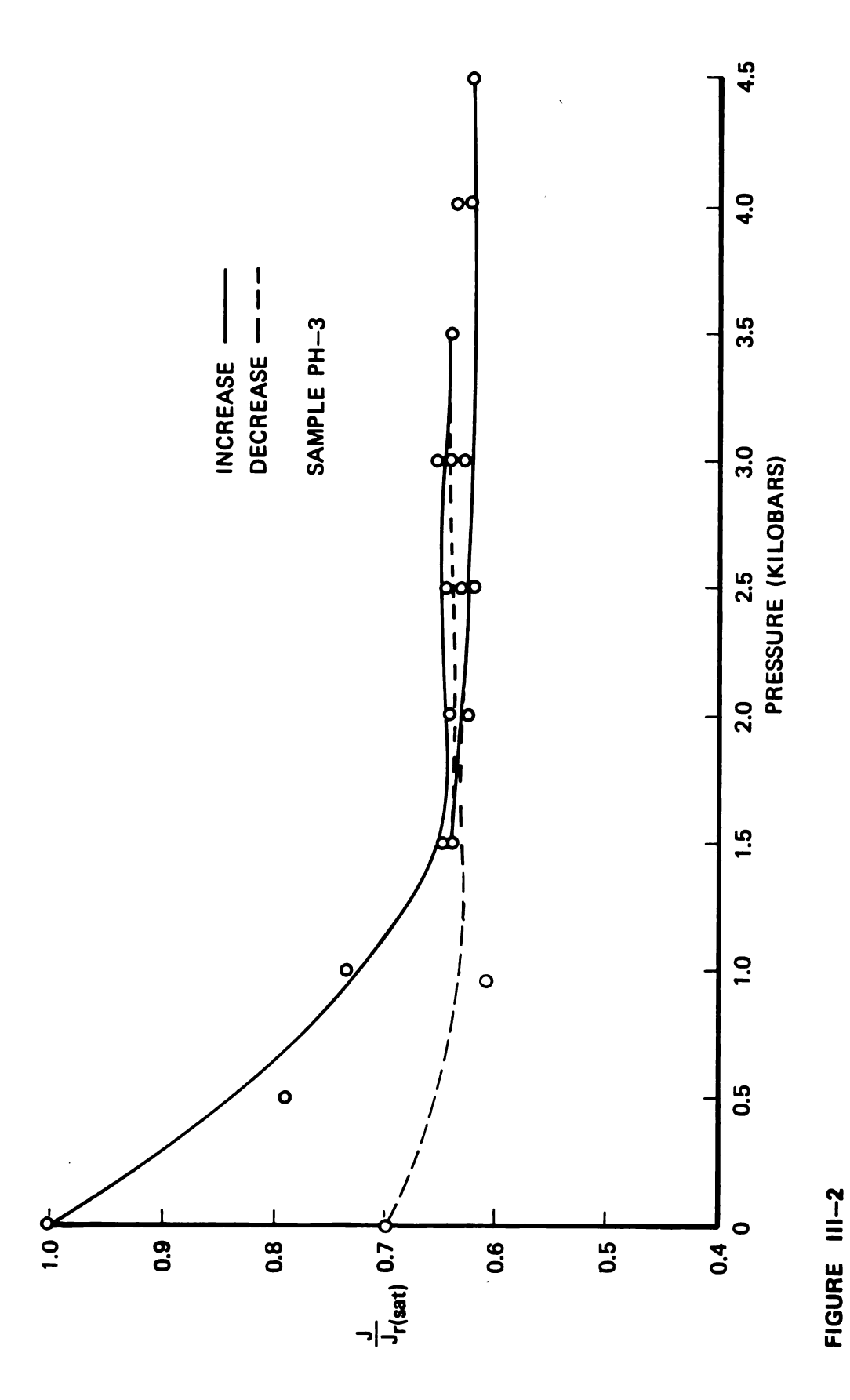
(from Carmichael, 1975)

Table 1.



MAGNETIZATION VS. PRESSURE

FIGURE 111-1



MAGNETIZATION VS PRESSURE

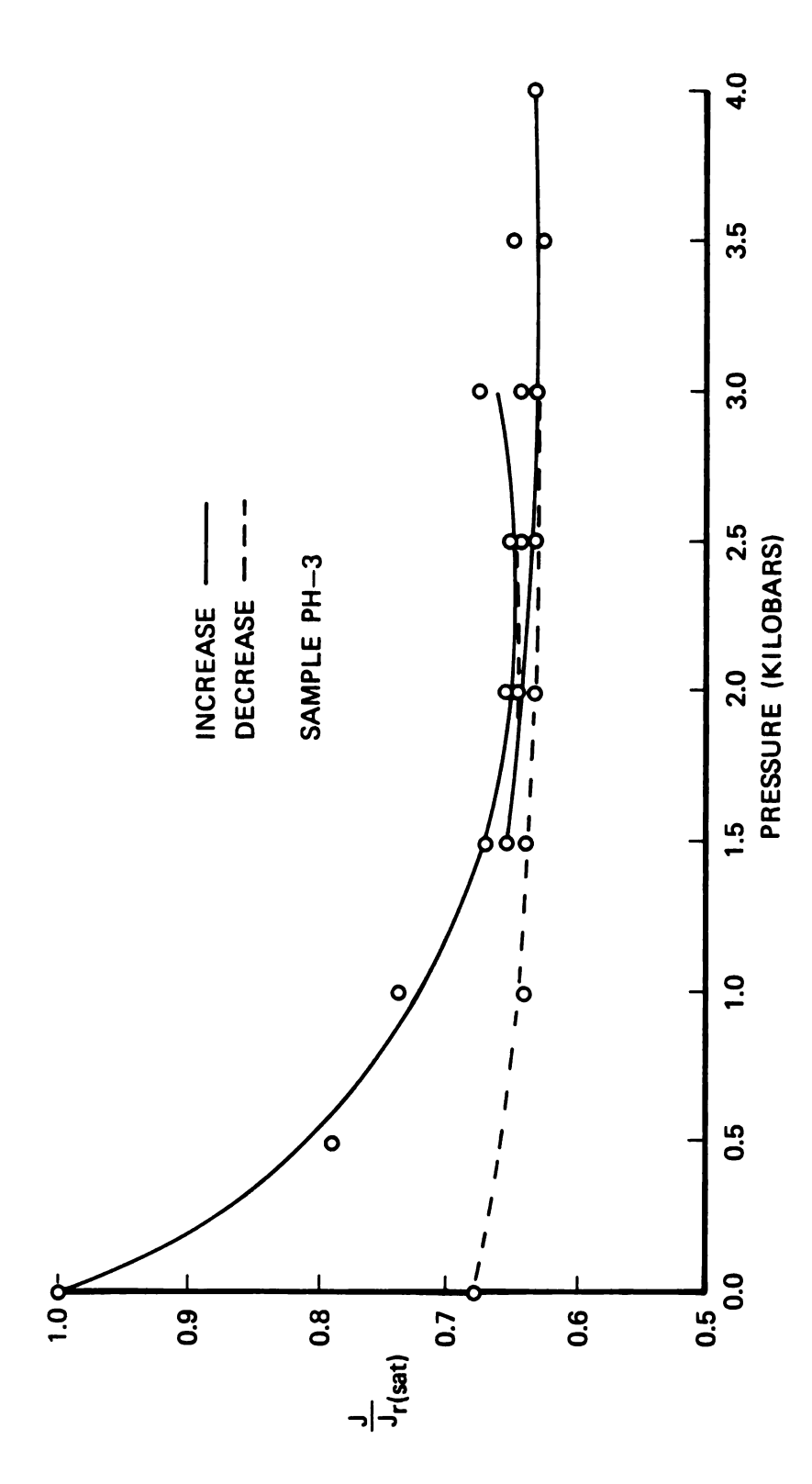
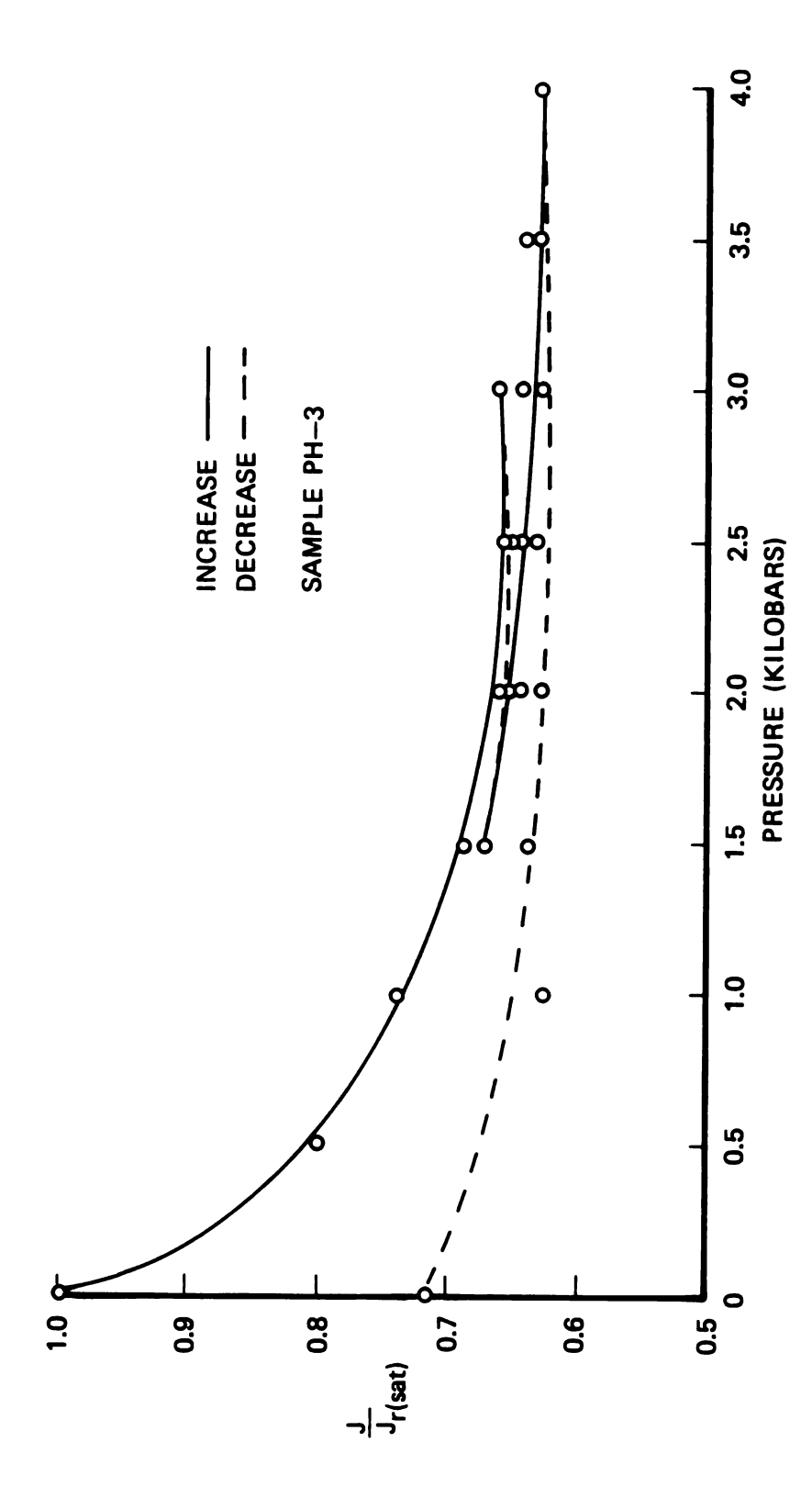


FIGURE III-3
MAGNETIZATION VS. PRESSURE



MAGNETIZATION VS. PRESSURE

FIGURE 111-4

V. INTERPRETATION

All samples experienced a sharp drop to approximately 66% of the initial saturation isothermal remanence from zero to 1.5 kilobars of applied pressure. This is similar to results obtained by Carmichael (1968) using applied uniaxial stress.

With the application of pressure, a certain amount of mechanical energy was input into the sample. Essentially, this added energy allows some domain walls to move over small potential energy barriers and relocate in new positions such that the domain energies more effectively cancel, thus decreasing the total grain energy. Since the pressurization took place in a zero field, the alteration of the sample in decreasing its total energy was also tending toward a net demagnetization.

The movement of domain walls under pressure occurs in both reversible and irreversible fashion. The net drop in J is a measure of the irreversible change; the difference between the minimum value of J (at maximum pressure) and the final value of J (at 1.0 kb) is a measure of the reversible change.

Some of the applied hydrostatic stress may have built up unevenly along existing flaws in the sample, such as along microcracks and irregularities in the lattice structure. This locally increased pressure would add a measure of directed stress, causing anisotropic effects. Such effects would induce altering the anisotropic energy terms K_1 and K_2

(in E_k). While an alteration of the "isotropic" energy, K_o , would not affect the domain configuration, changes in K_1 and K_2 would. Both amplitude and physical location of domain energy barriers in the region of locallized stress could be expected to change.

While such anisotropic changes in domain magnetization could occur, a random orientation of flaws within the sample would be expected to cancel any net change in the direction of magnetization. The resulting new domain configuration (after pressurization) was of lower energy than the initial configuration, with a greater degree of closure permitting a lower magnetization.

VI. CONCLUSION

Samples of magnetite were magnetically saturated and ubjected to hydrostatic pressurization to 4.0 kilobars. This is equivalent to the hydrostatic pressure in the crust at a depth of about 12 km. The isothermal remanent magnetization decreased with increased pressure to approximately 70% of the saturation value near 2.0 kb, at which point the magnetization appeared to stabilize. Subsequent cycling of the pressure to higher values failed to effect any noteworthy change in magnetization.

The results noted were probably due to the effects of the additional energy supplied to the samples by the pressurization. This new energy input to the magnetite grain allowed some domain walls to overcome small local potential energy barriers. These potential barriers had previously prevented the domains from aligning themselves in such a way as to minimize the total magnetic grain energy. Realignment of the domain walls and the subsequent alterations in domain configuration, allowed the grain energy to decrease, as noted in the magnetization drop. The irreversible effects are apparent in the net loss in J after pressurization (about a 30% $J_{r,sat}$ loss). Reversible effects may be noted in the rebound of the magnetization upon decompression of the last pressure cycle.

The results of the pressurizations have shown that the remanent magnetization of magnetite may be altered if the mineral

is or has been subjected to deep burial. Most of the pressure effect was observed at pressures less than 2 kilobars, corresponding to 6 km or about 20,000 feet (a depth to which some oil wells are drilled). Sampling magnetic properties of magnetic minerals cored from such wells could be worth future study.

Sufficient technology has now been developed and tested for measuring magnetic properties of rocks and minerals during pressurization. This is a distinct advancement over methods involving pressurization followed by separate measurements of magnetic properties. A suggested improvement would be a continuous monitoring of changes in magnetic properties during pressure cycling, as opposed to the discrete sampling currently in use.

APPENDIX

APPENDIX A

BOMB CALIBRATION DATA

Column A

Column B

Dial Force on Large Piston (x 1000 lb.)		Large Piston Position from Strain Gague (decreasing into chamber) (1.0 unit = 0.02 inches)	
A	В	A	В
11.5	15.10	7.5	15.74
12.0	14.82	7.0	16.12
12.6	14.30 TRANSITION	6.5	16.50
12.7	12.97	6.0	17.00
12.9	12.83	9.0	16.00
13.0	12.74	11.5	15.15
13.1	12.65	12.1	14.85
13.5	12.45	12.5	14.58 } TRANSITION
14.0	12.20	13.1	13.16 TRANSTITON
14.3	12.10	10.0	13.41
13.5	12.11	9.7	13.45
13.0	12.14	9.2	13.52
12.5	12.18	8.7	13.68
12.0	12.23	8.3	13.90 } TRANSITION
11.5	12.27	8.0	14.85 TRANSTITON
11.0	12.35	7.7	15.18
10.5	12.50	7.5	15.30
10.0	12.70	7.0	15.68
9.5	12.94	6.5	16.08
9.0	13.22 } TRANSITION		
8.5	15.15		
8.0	15.37		

BIBLIOGRAPHY

BIBLIOGRAPHY

- Banerjee, S.K., New grain size limits for paleomagnetic stability in hematite: <u>Nature Physical Sci.</u>, v. 232, pp. 15-16, 1971.
- Brace, W.F., A.S. Orange, and T.R. Madden, The effect of pressure on the electrical resistivity of water-saturated crystalline rocks: <u>J. Geophys. Res.</u>, v. 70, pp. 5669-5678, 1965.
- Breiner, S., and R.L. Kovach, Local geomagnetic events associated with displacements on the San Andreas Fault: Science, v. 158, no. 3797, pp. 116-118, 1966.
- Carmichael, R.S., Remanent and transitory effects of elastic deformation of magnetite crystals: Phil. Mag., v. 17, no. 149, p. 911-927, 1968.
- ----, Stress control of magnetization in magnetite and nickel, and implications for rock magnetism: J. Geomag. Geoelec., v. 20, no. 3, 1968a.
- ----, Hydrostatic pressurization of magnetite: Geophysics, v. 34, pp. 775-779, 1969.
- ----, Apparatus and results for pressure research on magnetic properties of magnetite, nickel and cobalt:

 <u>Coll. Intern. Centre Nat. Recherche Sci</u> (Paris)., no. 188, pp. 499-503, 1970.
- ----, "Paleomagnetism: A Laboratory Manual", Exploration Research Center, Shell Development Company, Houston, 1971.
 ----, Personal communication, 1975.
- ----, A. Sawaoka, and N. Kawai, A multipurpose high pressure microbomb: Jap. J. App. Phys., v. 7, pp. 1120-1124, 1968.
- Chikazumi, S., Physics of Magnetism, Wiley, New York, 1964.
- Clark, S.P., ed., <u>Handbook of Physical Constants</u>, G.S.A. Mem. 97, 1966.

- Craik. D.J., and R.S. Tebble, Ferromagnetism and Ferro-Magnetic Domains, Wiley, New York, 1965.
- Davis, P.M., and F.D. Stacey, Geomagnetic anomalies caused by a man-made lake: Nature, v. 240, 1971.
- Dobrin, M., Geophysical Prospecting, McGraw-Hill, New York, 1960.
- Dunlop, D.J., Magnetite: behavior near the single domain threshold: Science, v. 176, pp. 41-43, 1972.
- v. 162, no. 3850, pp. 256-258, 1968.
- ----, Superparamagnetic and single domain threshold sizes in magnetite: J. Geophys. Res., v. 78, pp. 1780-1793, 1973.
- ----, M. Ozima, and H. Kinoshita, Piezomagnetization of single domain graints: a graphical approach: J. Geomag. Geoelec., v. 21, no. 2, pp. 513-518, 1969.
- Golovkov, V.P., Anomalous geomagnetic field variations in a seismically active region: Geomag. and Aeronom., v. 6, 1969.
- Irving, E. Paleomagnetism and its application to geological and geophysical problems, Wiley, New York, 1964.
- Johnston, M.J.S., Tectonomagnetic effects: in <u>Proc. of</u>
 T. <u>Nagata Conference</u>, Goddard Space Flight Center,
 Greenbelt Md., 1975.
- Kawai, N., and A. Sawaoka, Magnetic measurements under hydrostatic pressure: intensity of J and anisotropy: Rev. Sci. Inst., v. 38, no. 12, pp. 1770-1772, 1967.
- Kim, K.T., Analysis of pressure generated in a pistoncylinder type apparatus: <u>J. Geophys.</u> Res., v. 79, pp. 3325-3333, 1974.
- Kinoshita, H., and T. Nagata, Dependence of magnetostriction and magnetocrystalline anisotropy of magnetite on hydrostatic pressure: <u>J. Geomag</u>, <u>Geoelec.</u>, v. 91, no. 1, pp. 77-79, 1967.
- Kittel, C., <u>Introduction</u> to <u>solid</u> <u>state</u> <u>physics</u>, Wiley, New York, 1965.
- Phys., v. 21, no. 4, pp. 541-583, 1949.

- Mason, B., and L.G. Berry, <u>Elements</u> of <u>mineralogy</u>, Freeman, San Francisco, 1968.
- Mirwald, P.W., I.C. Getting, and G.C. Kennedy, Low-friction cell for piston-cylinder high-pressure apparatus, J. Geophys. Res., v. 80, pp. 1519-1525, 1975.
- Nagata, T., Rock magnetism, rev. ed. Maruzen, Tokyo, 1961.
- ----, Principles of the ballistic magnetometer for the measurements of remanence: Methods in paleomagnetism, pp. 105-114, 1967.
- ----, Tectonomagnetism: IAGA Bull. No. 26, 1969.
- Neel, L., Some theoretical aspects of rock magnetism: Adv. Phys., v. 4, pp. .91-255, 1955.
- Paul, W., G. Benedek, and D. Warschaurer, Non-magnetic highpressure vessels: Rev. Sci. Inst., v. 30, no. 10, pp. 874-880, 1959.
- Rikitake, T., Geomagnetism and earthquake prediction: Tectonophysics, v. 6, p. 59, 1968.
- Sawaoka, A., and N. Kawai, Change of magnetic anisotropy constant K of magnetite under hydrostatic pressure: Phys. Let., v. 24a, no. 10, p. 503, 1967."
- ----, Effect of hydrostatic pressure on the magnetic anisotropy of ferrous and ferric ions in ferrites with spinel structure: J. Phys. Soc. Japan., v. 25, no. 1968.
- Schult, A., Effect of pressure on the curie temperature of titanomagnetites: Earth and Plan. Sci. Let., v. 10, 1970.
- Shimuda, M., S. Kume, and M. Koizumi, Demagnetization of unstable remanent magnetization by application of pressure: Geophys. J. Roy. Astr. Soc., v. 16, pp. 369-373, 1968.
- Soffel, H., The single domain--multi-domain transition in natural intermediate titanomagnetites: Zeit. Geophys., v. 37, pp. 451-470, 1971.
- magnetite: Zeit. Geophys., v. 32, pp. 63-77, 1966.
- Stacey, F.D., The physical theory of rock magnetism: Adv. Phys., v. 12, pp. 45-133, 1963.

- Stacey, F.D., and Banerjee, S.K., Physical principles of rock magnetism, Elsivier, New York, 1974.
- Stesky, R., and W.F. Brace, Electrical conductivity of serpentinized rocks to 6 kilobars: <u>J. Geophys. Res.</u>, v. 78, pp. 7614-7621, 1973.
- Wyllie, P.J., High-pressure techniques: Methods and techniques in geophysics, S.K. Runcorn, ed., Wiley, New York, 1966.
- Zijlstra, H., <u>Experimental methods in Magnetism</u>, (2. <u>Measure-ment of Magnetic quantities</u>), North-Holland, <u>Amsterdam</u>, 1967.

MICHIGAN STATE UNIVERSITY LIBRARIES

3 1293 03145 0442